ResearchGate

See discussions, stats, and author profiles for this publication at: https://www.researchgate.net/publication/248842754

Smectic A phase in a new bent-shaped mesogen based on a 2,3-naphthalene central core with an acute-subtended angle

ARTICLE *in* JOURNAL OF MATERIALS CHEMISTRY · APRIL 2010

Impact Factor: 7.44 · DOI: 10.1039/b919404e

CITATIONS
12

READS
27

7 AUTHORS, INCLUDING:

Ji-Hoon Lee
Chonbuk National University
60 PUBLICATIONS **306** CITATIONS

SEE PROFILE

Available from: Ji-Hoon Lee
Retrieved on: 17 January 2016

View Online

Smectic A phase in a new bent-shaped mesogen based on a 2,3-naphthalene central core with an acute-subtended angle

E-Joon Choi,*[a] Xin Cui,[a] Chang-Woo Ohk,[b] Wang-Cheol Zin,[b] Ji-Hoon Lee,*[c] Tong-Kun Lim[c] and Won-Gun Jang[d]

Received 17th September 2009, Accepted 17th February 2010
First published as an Advance Article on the web 9th March 2010
DOI: 10.1039/b919404e

Downloaded by Pohang University of Science and Technology on 27 December 2010
Published on 09 March 2010 on http://pubs.rsc.org | doi:10.1039/B919404E

A new bent-shaped molecule which consists of an acute-angled central core and all-ester linking groups has been prepared: 2,3-naphthylene bis[4-(4-n-dodecyloxybenzoyloxy)benzoate]. Its mesomorphic properties have been investigated by DSC, polarizing microscopy, and X-ray diffraction measurements. Moreover, we have carried out detailed electro-optical investigations including birefringence, switching current response, IR dichroism, and second-harmonic generation (SHG) measurements. On the basis of the experimental data a plausible model for the mesophase alignments has been proposed.

Introduction

Vorländer[1] was a pioneer who first described the synthesis and liquid crystalline properties of bent-shaped molecules with obtuse- and acute-angled configurations. Nowadays achiral bent-shaped mesogens have become an important field of liquid crystals and their structure-property relationships have been extensively studied.[2–8] In general, there are two main types of linking groups in bent-shaped mesogens: one contains Schiff's base linkages, and the other consists entirely of ester linkages. In most cases, these bent-shaped mesogens consist of five benzene rings including a 1,3-phenylene central core. Meanwhile, a limited number of bent-shaped compounds containing a naphthalene central core have been reported as compared to the 1,3-phenylene central core. There are two categories of bending angle of the naphthalene central core: one is based on the obtuse-subtended angle (120°) such as 1,3-, 1,6- and 2,7-dihydoxynaphthylenes, and the other the acute-subtended angle (60°) such as 1,2-, 1,7- and 2,3-dihydroxynaphthylene. The first bent-shaped compounds prepared from 2,7-dihydroxynaphthalenes by Shen *et al.*[9] did not show mesomorphic properties. At the same time, Pelzl *et al.*[4] reported that bent-shaped compounds without Schiff's base linkages derived from 2,7-dihydroxynaphthylene showed a B_1 phase. Several bent-shaped compounds with Schiff's base linkages were derived from 2,7-dihydroxynaphthalene, which exhibited smectic phases.[10–12] Reddy *et al.*[13,14] reported that homogeneous series of bent-shaped compounds with lateral fluorine substituents based on 2,7-dihydoxynaphthalene exhibited a nematic phase and B phases. Svoboda *et al.*[15] reported that some symmetrical and non-symmetrical bent-shaped mesogens with Schiff's base linkages based on 2,7-dihydroxynaphthalene showed a nematic phase and B phases. Recently, Rahman *et al.*[16] reported that bent-shaped monomers consisting of a 2,7-naphthalene central core and two vinyl end groups showed a nematic phase. Also, Novikova *et al.*[17] reported that bent-shaped ester compounds with lateral bromine substituents derived from 2,7-dihydroxynaphthalene showed B phases only for the long homologues. Most recently, Kohout *et al.*[18] reported that bent-shaped ester compounds based on a 7-hydroxynaphthalene-2-carboxylic acid showed a B2 phase and columnar smectic phases.

In the last few years, only a few articles have been devoted to the study of the bent-shaped mesogens based on the naphthalene central core with different substitution positions from the 2,7-dihydroxynaphthalene. Matsuzaki *et al.*[19] first reported that bent-shaped compounds based on 2,3-dihydroxynaphthalene with Schiff's base linkages could form nematic and smectic phases. Recently, a smectic A phase and B phases were found in bent-shaped molecules based on 1,2-, 1,3-, 1,6-, and 2,3-dihydroxynaphthalenes with Schiff's base linkages.[20] More recently, a phase sequence of N-SmA-$SmAP_A$-B4 was found in eight ring bent-shaped molecules based on a 1,7-dihydroxynaphthalene with Schiff's base linkages.[21] In our previous research we dealt with six ring bent-shaped mesogens based on 1,6- and 1,7-dihydroxynaphthalenes without Schiff's base linkages.[22] We found that the 1,7-compound was non-liquid crystalline, while the 1,6-compound could form a SmC_AP_A phase in the zero-field state, which switches to SmC_SP_F upon applying an electric field.

The main goal of this paper is to study the influence of an acute-angled central core on the mesomorphic behavior of bent-core mesogens with all-ester linkages. For this reason we have synthesized a new bent-shaped compound based on 2,3-dihydroxynaphthylene (Fig. 1), and its mesomorphic properties were investigated by DSC, polarizing microscopy and X-ray diffraction as well as various electro-optical measurements.

Experimental

Synthesis

2,3-Naphthylene bis[4-(4-n-dodecyloxybenzoyloxy)benzoate] was prepared by a modification of the procedure previously reported by our group.[23] The purity and structure of the final compound

[a]*Department of Polymer Science and Engineering, Kumoh National Institute of Technology, Gumi, Gyungbuk, 730-701, Korea. E-mail: ejchoi@kumoh.ac.kr; Fax: +82544787710; Tel: +82544787684*
[b]*Department of Material Science and Engineering, Pohang University of Science and Technology, Pohang, Gyungbuk, 790-784, Korea*
[c]*Department of Physics, Korea University, Seoul, 136-713, Korea*
[d]*Korea Photonics Technology Institute, Gwangju, 500-460, Korea*

View Online

Downloaded by Pohang University of Science and Technology on 27 December 2010
Published on 09 March 2010 on http://pubs.rsc.org | doi:10.1039/B919404E

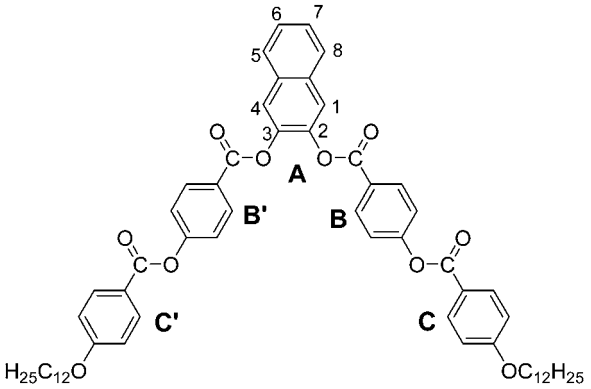

Fig. 1 Structural formula of the bent-shaped mesogen.

were confirmed by thin-layer chromatography, elemental analysis, and FT/IR and ^{1}H NMR spectrometry. The resultant data were in accordance with the expected formula. Yield: 43%. Density: 0.979 g/cm^3. FT/IR (KBr pellet, cm^{-1}): 3050–3150 (sp^2 C–H stretch), 2850 (sp^3 C–H stretch), 1740 (conj. C=O stretch), 1590 (C=C stretch), 1259, 1160 (C–O stretch). ^{1}H NMR (s = $CDCl_3$, δ in ppm): 8.17–7.99 (m, 8H, Ar-H), 7.76 (s, 2H, Ar-H), 7.20 (Ar-H: overlapping with the solvent peak), 7.05 (s, 2H, Ar-H), 6.95 (d, J = 8.5 Hz, 6H, Ar-H), 4.02 (t, J = 6.05 Hz, 4H, OCH_2), 1.81 (s, 4H, OCH_2CH_2), 1.48–1.25 (m, 36H, $O(CH_2)_2(CH_2)_9$), 0.86 (t, J = 6.15 Hz, 6H, $O(CH_2)_{11}CH_3$); ^{1}H NMR (s = CF_3CO_2D, δ in ppm): 8.20 (dd, J = 9.72, 5.87 Hz, 8H, Ar-H), 7.84 (s, 2H, Ar-H), 7.67 (s, 2H, Ar-H), 7.30 (d, J = 8.85 Hz, 4H, Ar-H), 7.07 (d, J = 8.94 Hz, 4H, Ar-H), 4.20 (t, J = 7.09 Hz, 4H, OCH_2), 1.87–1.83 (m, 4H, OCH_2CH_2), 1.26–1.07 (m, 36H, $O(CH_2)_2(CH_2)_9$), 0.88 (t, J = 10.7 Hz, 6H, $O(CH_2)_{11}CH_3$). Anal. Calcd for $C_{62}H_{72}O_{10}$: C 76.20, H 7.43; Found: C 76.22, H 7.50%.

Instrumentation

IR and NMR spectra were obtained using a Jasco 300E FT/IR and a Bruker DPX 200 MHz NMR spectrometer. Elemental analysis was performed with a Thermofinnigan EA1108. The transition behaviors were characterized using differential scanning calorimetry (Netzsch DSC 200 F3 Maia) and a polarizing microscope (Zeiss Axioskop 40 Pol) attached with a hot stage (Mettler FP82HT). DSC measurements were performed in a N_2 atmosphere with heating and cooling rates of 10 °C/min. The density was measured by a density gradient column procedure.

X-Ray measurements

XRD measurements were performed in transmission mode with synchrotron radiation at the 10C1 X-ray beam line (λ = 1.54 Å) at the Pohang Accelerator Laboratory (PAL) in Korea. On heating and cooling, the sample sealed with a window of 7 μm thick Kapton film on both sides was held in an aluminium sample holder. The data are presented as a function of $q = 4\pi\sin\theta/\lambda$ (θ: the scattering angle). The sample was heated with two cartridge heaters, and its temperature was monitored by a thermocouple placed close to the sample. A background scattering correction was performed by subtracting the scattering from the Kapton film.

Electro-optical investigations

The LC was injected between two ITO glass substrates by a capillary action at the isotropic phase (220 °C) of the sample. Each ITO deposited substrate was spin-coated with a commercial polyimide solution of (AL1254, JSR Corp.) and was baked for 1 h at 230 °C. The rubbing directions of the upper and the lower substrates were antiparallel to each other. The cell gap was 2 μm. A He-Ne laser (632 nm) was used to examine the electro-optical switching behavior of the cell. For the second harmonic generation (SHG) experiment, a Q-switched Nd-YAG pulse laser (GCR-200, Spectra Physics, 1064 nm, 7 ns pulse width, 10 Hz repetition rate) was used and the measurements were performed by using an experimental setup similar to one in the literature.[24] For the IR dichroism experiments, the absorption spectra of the sample were measured as a function of the rotating angle of the polarization of the incident IR beam using a FT-IR spectrometer (FTS-7700, Bio-Rad) and a ZnSe polarizer. The temperature of the sample was maintained within the accuracy of 0.1 °C using a heating stage (TMS94, Linkam).

Results and discussion

Thermal behaviour and microscopic textures

Fig. 2 shows DSC thermograms of the compound. The phase transition temperatures and associated enthalpy changes are given in Table 1. Three transition peaks for melting, mesophase 1-to-mesophase 2, and isotropization were found during cooling and heating. Phases were identified by optical/electrical, X-ray diffraction and SHG measurements. We could confirm that the compound forms a smectic A phase at lower temperature and a nematic phase at higher temperature.

Fig. 3 shows cross-polarizing optical micrographs obtained by using non-treated glass slides. When the isotropic liquid was cooled, no occurrence of birefringence was observed at the Iso-to-N transition temperature and then the nematic and smectic phases kept a homeotropic optical texture until crystallization (Fig. 3a). Interestingly, the homeotropic region could be supercooled during the cooling process (Fig. 3b). Reversibly, during the heating process, the smectic and nematic phases showed only a homeotropic optical texture.

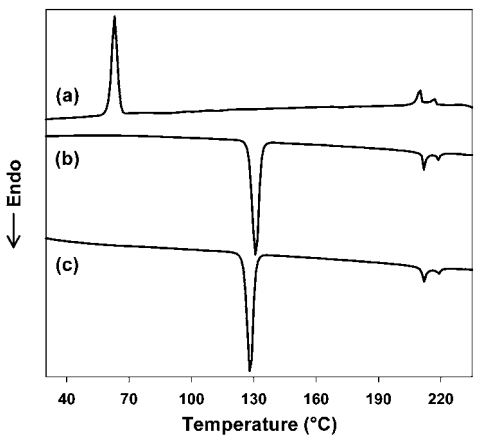

Fig. 2 DSC thermograms of the compound at a rate of 10 °C/min: during first heating (b), second heating (c) and first cooling (a) runs.

 This journal is © The Royal Society of Chemistry 2010

View Online

Downloaded by Pohang University of Science and Technology on 27 December 2010
Published on 09 March 2010 on http://pubs.rsc.org | doi:10.1039/B919404E

Table 1 Transition temperatures (°C) and enthalpy changes (kJ mol^{-1}, in parentheses)[a]

DSC run	Cr		SmA		N		Iso
1st heating	•	131 (45.1)	•	212 (2.7)	•	219 (0.8)	•
1st cooling	•	63 (32.7)	•	210 (2.9)	•	217 (0.7)	•
2nd heating	•	128 (43.9)	•	212 (2.6)	•	219 (0.8)	•

[a] Abbreviations: Cr = crystalline state; SmA = smectic A phase; N = nematic phase; Iso = isotropic liquid phase.

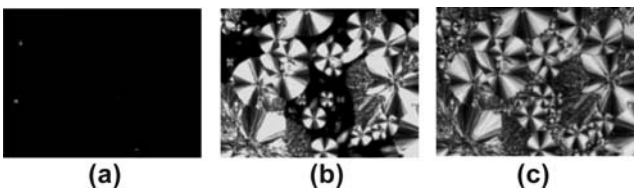

Fig. 3 Cross-polarizing optical micrographs during cooling (magnification ×200): (a) homeotropic optical texture of smectic A phase: $T = 192$ °C; optical textures of crystalline state: (b) $T = 57$ °C; (c) $T = 50$ °C.

X-Ray diffraction measurements

Fig. 4 shows the synchrotron radiation X-ray diffraction patterns obtained during heating and cooling. The mesophase was not surface-aligned and mounted between amorphous Kapton films. At room temperature and 100 °C, the compound shows many diffraction peaks (Fig. 4a and b). The scattering vectors of three peaks in the small angle region obey the ratio of 1 : 2 : 3. This is indicative of a well-defined lamellar crystalline structure with a layer thickness of 2.49 nm. On heating to 170–210 °C, a peak at $q = 1.88$ nm^{-1} appears in the small angle region, while all peaks in the wide angle region disappear (Fig. 4c–f). This is indicative of a smectic phase with a layer spacing of $d = 3.34$ nm. When further heated to 215 °C and 240 °C, only the broad scattering patterns were observed: these are indicative of a nematic phase (Fig. 4g) and an isotropic liquid phase (Fig. 4h), respectively. Subsequently, upon cooling from the isotropic liquid to 215 °C and 210 °C, a nematic phase appears reversibly (Fig. 4i and j). When cooled to 202 °C and 130 °C, a peak at $q = 1.84$ nm^{-1} ($d = 3.41$ nm) for a smectic phase appears (Fig. 4k and l). Upon further cooling to room temperature, many diffraction peaks were found (Fig. 4m). This crystalline state shows the optical texture with Maltese-cross spherulites shown in Fig. 3c.

To account for the stable conformation of the molecule in smectic A phase, we should consider the steric effect of the 2,3-naphthalene central unit whose second ring is extruded. In a similar way as the 1,3-phenylene central unit,[25,26] we have postulated that phenyl rings are coplanar with carbonyl groups attached to them, and alkyloxy groups in all-trans conformation are equiplanar to the benzene rings C or C′. However, the twist angle of the benzene rings B and B′ with respect to the benzene ring A should be larger than the case of 1,3-phenylene central unit. Based on the postulation, the molecular length was calculated to be about 3.4 nm, and the bending angle was estimated to be about 75°. Note that the magnitude of *d*-spacing of the smectic A phase was not dependent on temperature, while there was a subtle difference between the value (3.41 nm) on cooling and the value (3.34 nm) on heating. We assumed that the bending angle alters at higher temperature than $T_{N\text{-}Iso}$, so that the *d*-spacing during cooling can become different from that during heating.

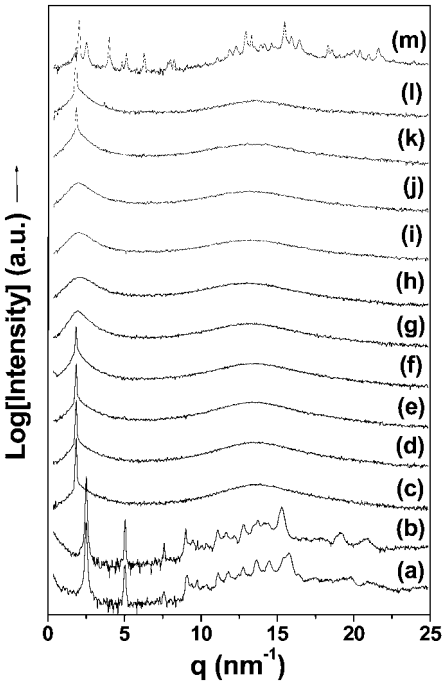

Fig. 4 Synchrotron radiation X-ray diffraction patterns: at (a) room temperature, (b) 100 °C, (c) 170 °C, (d) 198 °C, (e) 206 °C, (f) 210 °C, (g) 215 °C, and (h) 240 °C; as obtained by cooling from the isotropic liquid at (i) 215 °C, (j) 210 °C, (k) 202 °C, (l) 130 °C, and (m) room temperature. The *q* values (nm^{-1}) in the small angle region: 2.52 (a, b), 1.88 (c–f), 1.84 (k, l), 2.02, and 2.52 (m).

Electro-optical investigations

For electro-optical investigation, homogeneously aligned cells were used. The glass substrates with indium tin oxide (ITO) electrodes were coated with polyimide and rubbed antiparallel to each other. Fig. 5 shows cross-polarizing optical micrographs obtained at 160 °C. When the directions of polarizer (P) and analyzer (A) crossing each other make an angle of 45° with the rubbing direction (R), the cell shows strong birefringence with uniformly aligned surface (Fig. 5a). When the P (or A) is parallel to the R, the cells show no birefringence (Fig. 5b). This strongly implies that the homogeneous alignment condition for the nematic phase of rod-like mesogens could lead the smectic A phase of V-shaped mesogen to have a planar alignment. Note that in Fig. 5 there is no cell response to the field. Interestingly, when an electric field of 40 V μm^{-1} dc was applied along the surface normal direction, only a dark state was induced. This means that upon treatment with a 40 V μm^{-1} dc field, the birefringent state can be switched into the non-birefringent state. Once it happened, such a dark state remained even after removal of the 40 V μm^{-1} dc field. Only after thermal refreshment, which is subjected to reaching an isotropic state, could the initial birefringence state be obtained again.

View Online

Downloaded by Pohang University of Science and Technology on 27 December 2010
Published on 09 March 2010 on http://pubs.rsc.org | doi:10.1039/B919404E

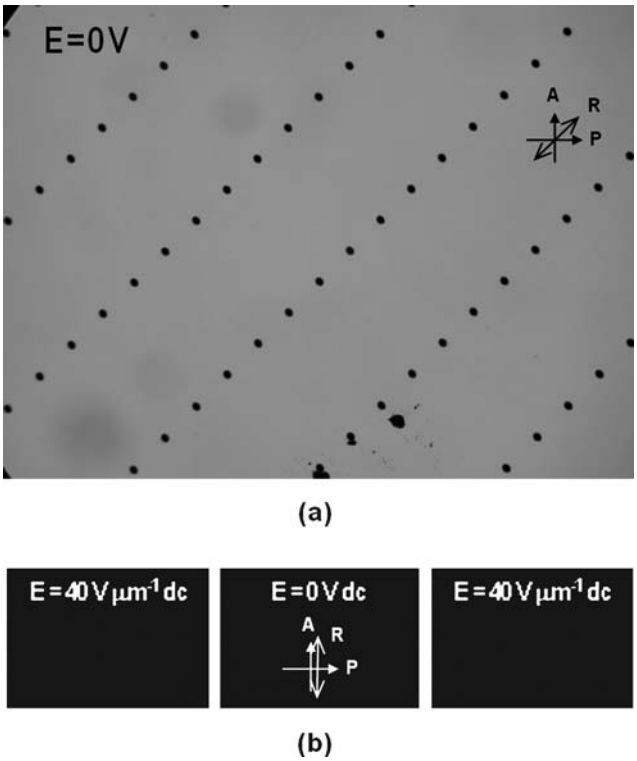

Fig. 5 Cross-polarizing optical micrographs: the glass substrates with ITO electrodes were coated with polyimide (AL 1254; JSR) and were rubbed antiparallel to each other ($T = 160$ °C; $d = 2$ μm). (a) The angle between crossed polarizers (P and A) and rubbing direction (R) is 45°. (b) The angle between P (or A) and R is 0°.

Fig. 6 shows the optical transmittance as a function of rotation angle of a set of crossed polarizers. The probe beam was normally incident, and the output beam intensity was measured while a crossed polarizer is rotating. At field-off state as well as at a triangular electric field-on state, the angle at the maximum transmittance was set to be 0°, and then the minimum transmittance was observed at the angle of ±45° (Fig. 6a and b). This means the optical axis of the cell is oriented parallel to the rubbing direction. When an electric field of 40 V μm^{-1} dc was applied, only a trace of birefringence was observed (Fig. 6c). Such a dark state lasted after removing the 40 V μm^{-1} dc field (Fig. 6d) and then during applying another triangular electric field (Fig. 6e). The results indicate that the optical axis of the smectic A phase was not changed by applying an external electric field.

Fig. 7 shows the polarized IR absorption profile of the sp^3 C–H stretch as a function of the angle between the rubbing direction and the polarization direction of incident IR light. When the polarization direction was parallel to the rubbing direction, maximum IR absorption was observed, while when the polarization direction was perpendicular to the rubbing direction, minimum absorption was found. Upon application of an electric field, the IR profile stayed almost the same. This provides evidence for a smectic A phase where the principal axis of the bent-shaped molecule with acute-angled configuration can homogeneously align along the rubbing direction.

Figs 8 and 9 show the triangular electric field dependences of switching current and optical transmittance response, respectively. Initially, the polarization direction was set to make an

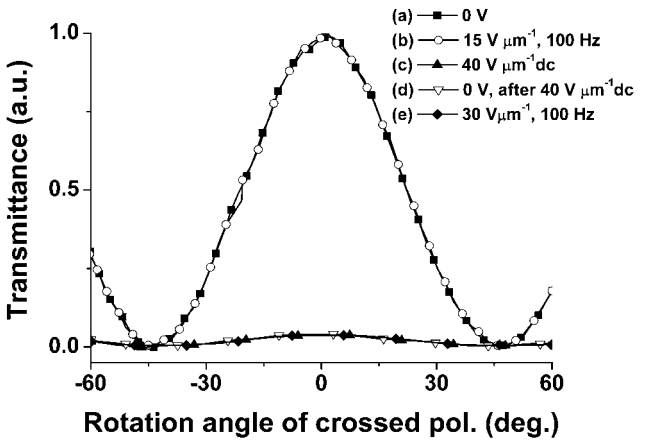

Fig. 6 Optical transmittance as a function of rotation angle of crossed polarizer ($T = 160$ °C): (a, b) intermediate field state; (c–e) strong field state.

angle of 45° with the rubbing direction. Before the 40 V μm^{-1} dc field treatment, by applying a triangular electric field, a single reverse current peak was recorded every half period indicating a ferroelectric-like switching (Fig. 8), whereas the optical transmittance of the phase was not changed at all. In contrast, after the 40 V μm^{-1} dc field treatment, under application of a triangular electric field, an optical switching was recorded (Fig. 9). In Fig. 8, the threshold voltage for the polarization switching seems to increase with the applied voltage. We think this is caused by an internal polarization charge of the bent-core molecules. Because the LC molecules seem to have a strong dipole moment, it can make a strong polarization charge inside of the cell and this makes a local electric field inside of the cell. Stronger electric field induces more uniform alignment of LC dipoles, and then the local field also increases. Accordingly, the effective electric field (= external electric field − local electric field) should reduce as the applied electric field increases. As a result, the threshold voltage of switching should increase with stronger applied voltage. In Fig. 9, under the extremely strong voltage applied, the LC cell was switched into an optically isotropic state where the direction of the principal molecular axis may become almost

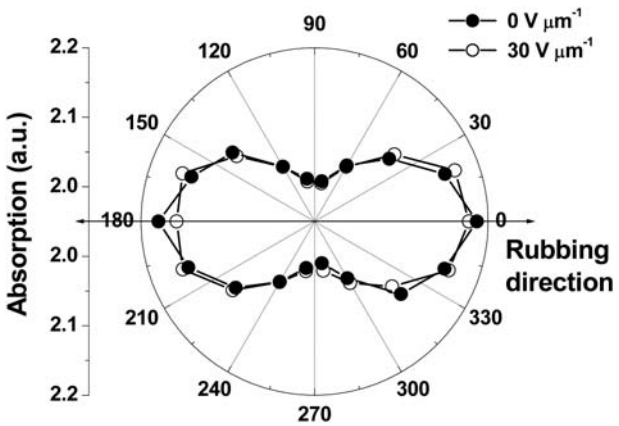

Fig. 7 Polarized IR absorption profile ($1/\lambda = 2852$ cm^{-1}) as a function of polarization angle with/without application of an electric field ($f = 100$ Hz): the ZnSe substrates with ITO electrodes were coated with polyimide and were rubbed ($T = 160$ °C).

 This journal is © The Royal Society of Chemistry 2010

View Online

Downloaded by Pohang University of Science and Technology on 27 December 2010
Published on 09 March 2010 on http://pubs.rsc.org | doi:10.1039/B919404E

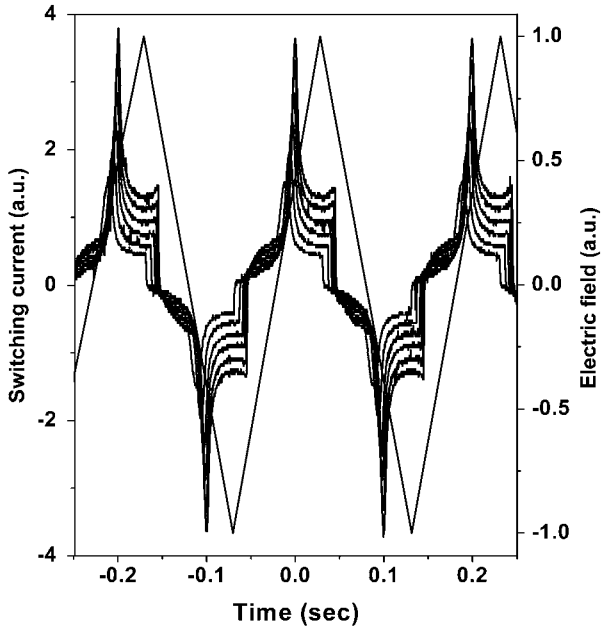

Fig. 8 Switching current response by applying a triangular electric field at intermediate field state ($T = 160$ °C; $f = 5$ Hz). As an electric field of 10, 15, 20, 25, 30 and 35 V μm^{-1} was applied, the curve intensity increases in that order.

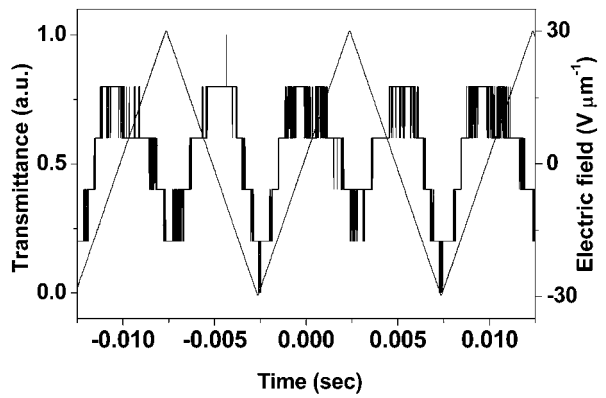

Fig. 9 Optical transmittance by applying a triangular electric field at strong field state ($T = 160$ °C; $E = 40$ V μm^{-1} dc; $f = 100$ Hz).

parallel to the direction of the polarizer, but not perfectly, and thus showed a very small optical switching response by rotation around the principal molecular axis.

In Fig. 10, the polarization calculated from the switching current response is plotted as a function of applied electric field. In the homogeneously aligned cell, the polarization shows a sudden rise at 1.0 V μm^{-1}. This indicates that the molecular rotation around the principal axis must overcome the threshold voltage (E_{th}). When these data are fit to a linear line in this field regime, a field-independent polarization was deduced to the magnitude of about 65 nC cm^{-2}. This means that there are both field-induced and field-independent polarizations in the system. In other words, the dipoles of LC molecules are randomly aligned at zero field state and are switched to a uniformly aligned state with a spontaneous polarization. Once switched to such a polar state over a threshold, then the LCs are switching holding the spontaneous polarization.

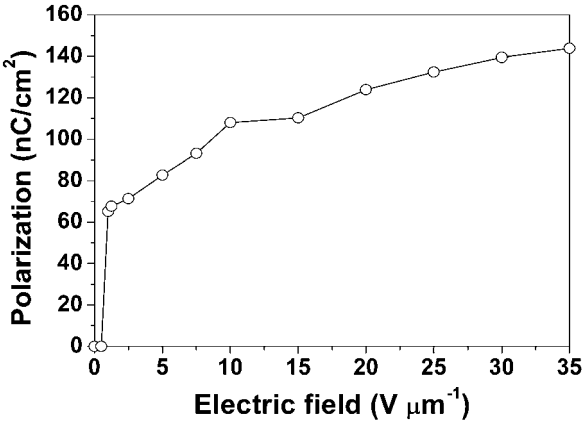

Fig. 10 Plot of polarization calculated from current response *vs.* applied electric field.

Fig. 11 shows the effect of applied voltage on the SHG intensity. A polarized probe beam struck the *xz* plane with an incident angle of 32°: the projected polarization direction of polarizer and analyzer on the cell surface was parallel to the rubbing direction ($\hat{x}$). At zero-field state no SHG signal was detected. As a field of 1.2 V μm^{-1} was applied, the SHG intensity showed a sudden rise and then increased gradually. The SHG intensity almost did not show a hysteresis depending on the field strength. The results imply that in the homogeneously aligned cell, a non-polar smectic A phase can be switched into a polar smectic A phase (SmAP) by applying a stronger field than the E_{th}.

Fig. 12 shows the polar plot of SHG intensity generated by an obliquely incident pump beam with an incident angle of 32° in the *yz*-plane: the mirror plane corresponds to the *xz*-plane. The SHG signal was measured with a triangular electric field. The ϕ_p and ϕ_a are the angles at which the projected directions of the polarizer and the analyzer on the *xz* plane join the $\hat{z}$ axis in the *yz*-plane, respectively. Two leaf SHG patterns occur when the polarizer was rotated with the analyzer fixed to the $\hat{z}$ direction (ϕ_p, 0°) as well as when the analyzer was rotated with the polarizer fixed to the $\hat{z}$ direction (0°, ϕ_a). Four leaf SHG patterns occur when the polarizer was rotated with the analyzer fixed to

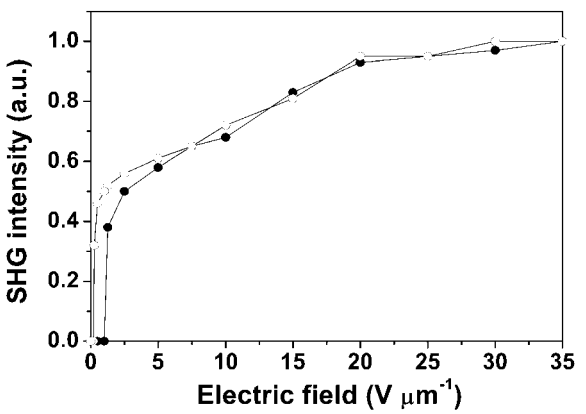

Fig. 11 SHG intensity as a function of applied electric field ($T = 160$ °C; $f = 100$ Hz). Open circles: course of voltage increase; filled circles: course of voltage decrease.

View Online

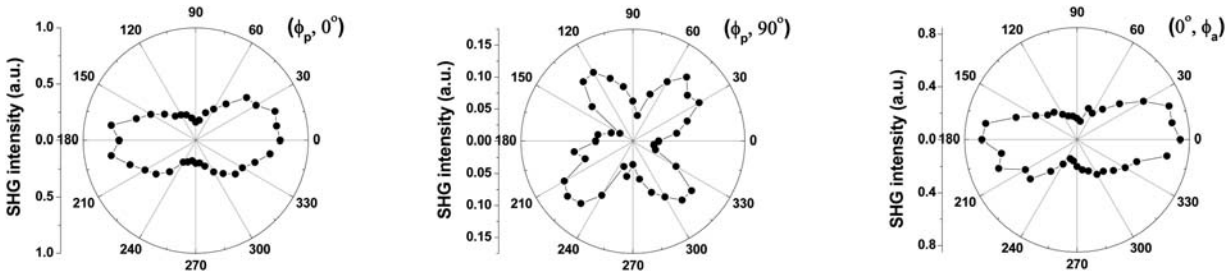

Fig. 12 Polar profile of SHG intensity by applying a triangular electric field ($E = 30$ V μm^{-1}; $f = 100$ Hz; $T = 160$ °C).

Downloaded by Pohang University of Science and Technology on 27 December 2010
Published on 09 March 2010 on http://pubs.rsc.org | doi:10.1039/B919404E

the $\hat{x}$ direction (ϕ_p, 90°). This polar pattern of SHG intensity indicates that the overall point symmetry of the sample is C_{2v} or $C_{\infty v}$ (rotation axis: $\hat{z}$).[27,28] In our system, the symmetry of the phase was considered as C_{2v} because the optical birefringence data (Fig. 6) and IR dichroism data (Fig. 7) shows the principal axes of LC molecules are anisotropically oriented to the rubbing direction.

Conclusions

In summary, we discovered that a bent-shaped molecule with acute-subtended configuration (*ca.* 75°) with all-ester linkages could form a smectic A phase as well as a nematic phase. In addition, we could propose the alignment structures of mesophase as shown in Fig. 13. On the one hand, when no surface treatment was applied, the directors of LC molecules are aligned in orthogonal fashion to the surface where the dipoles are randomly oriented; this is optically isotropic for a normal incident probe beam (Fig. 13a). On the other hand, when the ITO surfaces were coated with polyimide and rubbed, planar LC structures were found (Fig. 13b–e): in the molecular frame, the director is parallel to the principal axis, and the dipole vertical to this axis; in the laboratory frame, the directors are parallel to the rubbing directions ($\hat{x}$), and the dipoles to the $\hat{z}$ axis. Without application of an electric field, the dipoles are randomly oriented along the $\hat{z}$ axis (Fig. 13b). When an intermediate electric field over a threshold is applied, the dipoles rotate around the $\hat{x}$ axis in the xz plane to be aligned along the $\hat{z}$ axis, namely, the field-induced orientation occurs based on the collective rotation of the molecules around their long molecular axes (Fig. 13c). Then the dipoles align to the field direction by switching $+z$ direction or $-z$ direction depending on the field direction (Fig. 13d). At this state, the LC molecules showed a polarization current and a second harmonic activity with no change of optical transmittance. As a result, we could confirm a polar smectic A phase with ferroelectric alignment ($SmAP_F$) is induced. The fixed mechanism needs further studies. Furthermore, when an extremely strong voltage (40 V μm^{-1} dc) is applied, the LC molecules seem to re-orient possibly to have a diagonal alignment to the rubbing direction which is optically isotropic (Fig. 13e). Then, this state could switch holding an almost optically isotropic character, because the direction of the

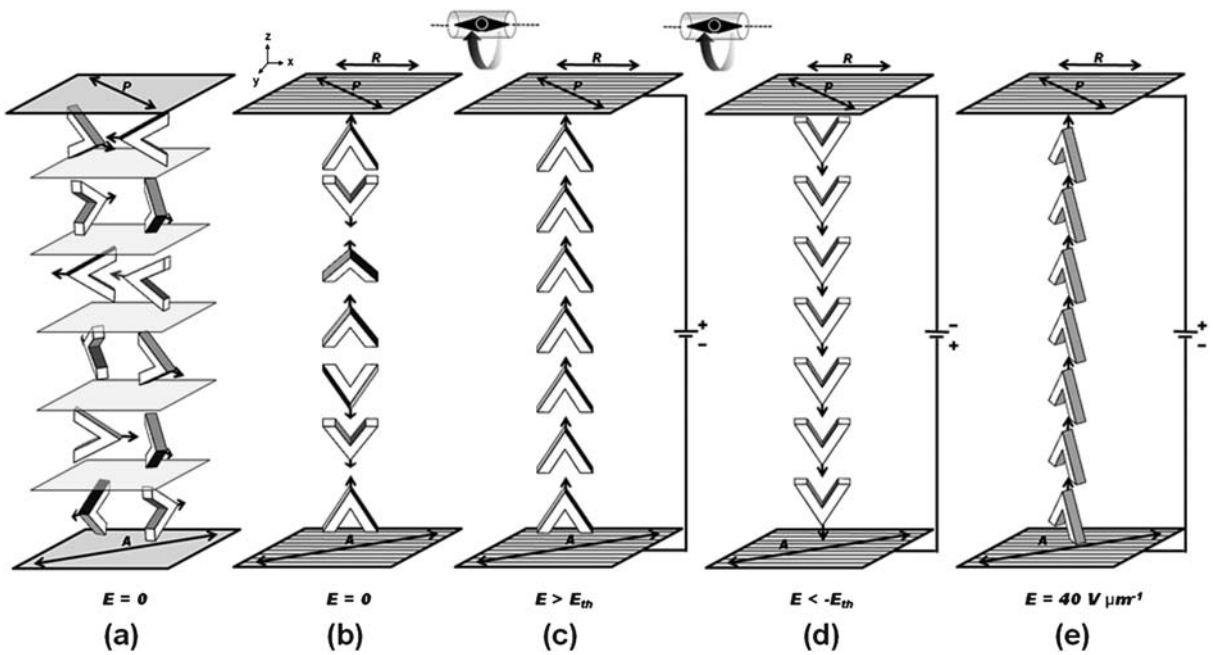

Fig. 13 A plausible model for alignments of smectic A mesophase. (a) A homeotropic LC structure in a cell without properly treated surfaces. (b–d) Planar LC structures in cells with homogeneous alignment substrates: ferroelectric alignment at intermediate field state (c, d); optically isotropic alignment at strong field state (e).

 This journal is © The Royal Society of Chemistry 2010

View Online

principal molecular axis is parallel to the direction of polarizer, but not perfectly, and rotation around the long molecular axis takes place. The exact mechanism is not fully understood in this isotropic state and more study is needed. Particularly, such a strong field state could be transformed into the intermediate field state only by thermal refreshment subjected to heating above the isotropization temperature.

Acknowledgements

This work was supported by the Korea Science and Engineering Foundation (KOSEF) grant funded by Korea government (MEST) (No. R01-2008-000-11521-0). E-J. C. wishes to express his sincere appreciation to Prof. D. M. Walba for critical discussion of the topic and valuable suggestions and comments. The authors would like to thank Y.-H. Seo for drawing Fig. 13.

References

1 D. Vorländer, *Ber. Dtsch. Chem. Ges. B*, 1929, **62**, 2831; D. Vorländer and A. Apel, *Ber. Dtsch. Chem. Ges. B*, 1932, **65**, 1101.
2 T. Niori, T. Sekine, J. Watanabe, T. Furukawa and H. Takezoe, *J. Mater. Chem.*, 1996, **6**, 1231.
3 D. R. Link, G. Natale, R. Shao, J. E. Maclennan, N. A. Clark, E. Korblova and D. M. Walba, *Science*, 1997, **278**, 1924.
4 G. Pelzl, S. Diele and W. Weissflog, *Adv. Mater.*, 1999, **11**, 707.
5 D. Shen, A. Pegenau, S. Diele, I. Wirth and C. Tschierske, *J. Am. Chem. Soc.*, 2000, **122**, 1593.
6 H. N. Shreenivasa Murthy and B. K. Sadashiva, *Liq. Cryst.*, 2002, **29**, 1223.
7 W. Weissflog, H. N. Shreenivasa Murthy, S. Diele and G. Pelzl, *Philos. Trans. R. Soc. London, Ser. A*, 2006, **364**, 2657.
8 H. Takezoe and Y. Takanishi, *Jpn. J. Appl. Phys.*, 2006, **45**, 597.
9 D. Shen, S. Diele, G. Pelzl, I. Wirth and C. Tschierske, *J. Mater. Chem.*, 1999, **9**, 661.
10 J. Thisayukta, H. Kamee, S. Kawauchi and J. Watanabe, *Mol. Cryst. Liq. Cryst.*, 2000, **346**, 63.
11 J. Thisayukta, Y. Nakayama and J. Watanabe, *Liq. Cryst.*, 2000, **27**, 1129.
12 J. Thisayukta, H. Niwano, H. Takezoe and J. Watanabe, *J. Mater. Chem.*, 2001, **11**, 2717; J. Thisayukta, Y. Nakayama, S. Kawauchi, H. Takezoe and J. Watanabe, *J. Am. Chem. Soc.*, 2000, **122**, 7441.
13 R. A. Reddy and B. K. Sadashiva, *Liq. Cryst.*, 2000, **27**, 1613.
14 R. A. Reddy and B. K. Sadashiva, *J. Mater. Chem.*, 2004, **14**, 1936.
15 J. Svoboda, V. Novotna, V. Kozmik, W. Weissflog, S. Diele and G. Pelzl, *J. Mater. Chem.*, 2003, **13**, 2104.
16 M. L. Rahman, J. Asik, S. Kumar and C. Tschierske, *Liq. Cryst.*, 2008, **35**, 1263.
17 N. S. Novikova, E. Gorecka, R. V. Kondratyeva and E. D. Kilimenchuk, *Liq. Cryst.*, 2008, **35**, 743.
18 M. Kohout, J. Svoboba, V. Novotná, D. Pociecha, M. Glogarová and E. Gorecka, *J. Mater. Chem.*, 2009, **19**, 3153.
19 H. Matsuzaki and Y. Matsunaga, *Liq. Cryst.*, 1993, **14**, 105.
20 S.-K. Lee, Y. Naito, L. Shi, M. Tokita, H. Takezoe and J. Watanabe, *Liq. Cryst.*, 2007, **34**, 935; S. K. Lee, M. Tokita, Y. Shimbo, K.-T. Kang, H. Takezoe and J. Watanabe, *Bull. Korean Chem. Soc.*, 2007, **28**, 2241.
21 S.-K. Lee, X. Li, S.-M. Kang, M. Tokita and J. Watanabe, *J. Mater. Chem.*, 2009, **19**, 4517.
22 E-J. Choi, X. Cui, W.-C. Zin, C.-W. Ohk, T.-K. Lim and J.-H. Lee, *ChemPhysChem*, 2007, **8**, 1919.
23 C.-K. Lee, A. Primak, A. Jákli, E-J. Choi, W.-C. Zin and L.-C. Chien, *Liq. Cryst.*, 2001, **28**, 1293; C. K. Lee, J.-H. Kim, E-J. Choi, W.-C. Zin and L.-C. Chien, *Liq. Cryst.*, 2001, **28**, 1749.
24 A. Yariv, *Optical Electronics in Modern Communications*, Oxford University Press, 1997.
25 K. Fodor-Csorba, A. Vajda, G. Galli, A. Jákli, D. Demus, S. Holly and E. Gács-Baiz, *Macromol. Chem. Phys.*, 2002, **203**, 1556.
26 W. Weissflog, Ch. Lischka, S. Diele, G. Pelzl, I. Wirth, S. Grande, H. Kresse, H. Schmalfuss, H. Hartung and A. Stettler, *Mol. Cryst. Liq. Cryst.*, 1999, **333**, 203.
27 T. Furukawa, H. Takezoe, T. Nishi, T. Mitsukuchi, A. Migita, J. Watanabe, T. Watanabe and S. Miyata, *Mol. Cryst. Liq. Cryst.*, 1997, **299**, 105.
28 J. Watanabe, L. Yuquing, H. Tuchiya and H. Takezoe, *Mol. Cryst. Liq. Cryst.*, 2000, **346**, 9.

Downloaded by Pohang University of Science and Technology on 27 December 2010
Published on 09 March 2010 on http://pubs.rsc.org | doi:10.1039/B919404E